Chem. Chem. Technol., 2019,
Vol. 13, No. 3, pp. 288–295

Chemistry

THE SYNTHESIS AND THEORETICAL ANTI-TUMOR STUDIES OF SOME NEW MONOAZA-10*H*-PHENOTHIAZINE AND 10*H*-PHENOXAZINE HETEROCYCLES

Efeturi A. Onoabedje[1], Sunday N. Okafor[2], Kovo G. Akpomie[1], Uchechukwu C. Okoro[1,*]

https://doi.org/10.23939/chcht13.03.288

Abstract. The synthesis and anticancer activity of a series of new 3-amido derivatives of 3-chloro-10*H*-pyrido[3,2-b][1,4]benzoxazine and 3-chloro-10*H*-pyrido [3,2-b][1,4]benzothiazine is presented. The synthesized structures were characterized by UV-visible, FT-IR, ^{1}H NMR spectroscopy and elemental analytical data. The *in silico* physicochemical properties disclosed that neither 3-chloro-10*H*-pyrido[3,2-b][1,4]benzoxazine and 3-chloro-10*H*-pyrido[3,2-b][1,4]benzothiazine intermediates nor their carboxyamido derivatives violate Lipinski's rule of five. In addition, molecular docking studies showed that they exhibited good interaction with cancer receptors. 1,3-di-10*H*-Pyrido[3,2-b][1,4]benzothiazin-3-ylurea which showed a significant interaction with all the employed receptors possessed the highest anticancer activity.

Keywords: synthesis, phenoxazine, phenothiazine, carboxyamide, anticancer, docking.

1. Introduction

Anticancer activity of new phenothiazine derivatives was extensively studied over the last two decades [1]. A variety of benzo and dibenzophenothiazine was known to display a promising anticancer activity [2, 3]. Pluta *et al.* [4] have recently described a significant anticancer activity of azaphenothiazines tested on 55–60 *in vitro* cell lines such as leukemia, non-small cell lung, colon, CNS, melanoma, ovarian, renal, prostate and breast cancers. The anticancer activity of the azaphenothiazines was attributed in part to the thiazine nitrogen in the molecules [4]. Also in recent times various derivatives of phenoxazine have been reported to possess multidrug resistance (MDR) modulator in cancer cells [5, 6]. The presence of phenoxazine nucleus in the structure of naturally occurring Actinomycin D antibiotic and anticancer produced by *Streptomyces* suggests synthesized derivatives of phenoxazine to be potential chemotherapeutic agents [7]. Kato [8] reported that 2-amino-4,4α-dihydro-4α,7-methyl-3*H*-phenoxazin-3-one and 2-aminophenoxazin-3-one were effective in the treatment of pancreatic cancer. In another development, Kapadia [9] demonstrated that the modification of phenothiazine and phenoxazine ring afforded derivatives which possess significant inhibition of *in vitro* Epstein-Barvirus early antigen (EBV-EA). Our earlier work also disclosed phenoxazines as antibiotic leading agents because of their potent inhibition of penicillin binding proteins (PBP) [10]. The inability of anticancer chemotherapeutic agents to selectively discriminate normal cell from cancerous cells as well as serious side effects of administering anticancer drugs constitutes the greatest challenge in cancer treatments [11]. Another major issue in a cancer therapy is the multidrug resistance effect of cancerous cells to numerous chemotherapeutic drugs which often result in treatment failure [12]. Therefore, dedicated effort towards evaluation of potential anticancer agents by medicinal chemists in view to find solutions of the aforementioned problems continued unabatedly.

Recently, metal-catalyzed amidation reactions of aryl halides have become an attractive protocol for synthesizing *N*-arylamides [13-16] and this had been utilized in accessing various azaphenoxazine carboxamides [17]. In this study, similar protocols were applied in the synthesis of new azaphenothiazine carboxy-amides as potential anticancer agents. The *in-silico* physicochemical properties and molecular docking studies of azaphenoxazine and azaphenothiazine carboxamides for anticancer drugs likeness were also described.

[1] Department of Pure & Industrial Chemistry, University of Nigeria, Nsukka, Nigeria
[2] Department of Pharmaceutical and Medicinal Chemistry, University of Nigeria, Nsukka, Nigeria
[*] *uchechukwu.okoro@unn.edu.ng*

2. Experimental

2.1. General Information

All chemicals were purchased from Sigma-Aldrich Chemical Company and were used without further purification. Melting points were determined with a Fischer-Johns apparatus and were uncorrected. ^{1}H and ^{13}C NMR data were recorded with Brucker DPX 400 MHz spectrometers relative to TMS as an internal standard. All chemical shifts were reported in ppm (δ) and coupling constants (J) reported in Hz. Multiplicity are indicated using the following abbreviations: br, for broad; s, for singlet; d, for doublet; t, for triplet; dd, for doublet of doublets and; m, for multiplet. Elemental analysis was carried out at the Central Science Laboratory, University of Cairo, Egypt on a CE440 Elemental Analyzer. UV-Visible Spectra were recorded on Cecil 7500 Aquarius 7000 Series Spectrometer at Chemistry Advance Laboratory (CAL), Sheda Science & Technology Complex (Shestco) Abuja, Nigeria, using matched 1 cm quartz cells and methanol as a solvent. Infrared spectral data were obtained on FT-IR-8400s using KBr disc and reported in wave number (cm^{-1}). The physicochemical properties were studied using Molinspiration Chemoinformatics softwares (http://www.molinspiration.com). The drug-likeness was evaluated using Lipinski's rule of five. In order to gain more insight about the binding modes of compounds **1**–**12**, docking studies were performed. Five cancer target proteins were chosen for this study and the 3D structures of these proteins were downloaded from the Protein Data Bank. They are Signaling protein [18] (PDB code: 3kkp) at the resolution of 1.35 Å; Mitotic regulator for chromosomal alignment and segregation (PDB code: 2x9e) at the resolution of 3.10 Å [19]; Oncogene protein [20] (PDB code: 5P21) at the resolution of 1.35 Å; Androgen receptor [21] (PDB code: 1gs4) at the resolution of 1.95 Å and RAS-RAF-mitogen activated protein kinase/extracellular signal-regulated kinase [18] (PDB code: 3PP1) at the resolution of 1.35 Å.

Human androgen receptor activity has been clearly linked to a prostate cancer. Prostate cancer cells, similar to normal prostate cells, require androgens to grow and survive [21]. However, inhibition of androgen receptor activity will ultimately prevent the production of androgens, and subsequently inhibits prostate cancer growth. Human Mitogen-activated protein kinase is one of the activators that mediates pathways for proliferative and anti-apoptotic signaling from growth factors and oncogenic factors leading to a tumor growth, progression, and metastasis [22] This, therefore, provides a molecular target for discovery of new anti-cancer drugs. Human monopolar spindle 1 (MPS1) kinase (2x9e) is a key regulator of the spindle assembly checkpoint (SAC). SAC is required for proper chromosomal alignment and segregation. This kinase has been found in a wide range of human tumors and is necessary for tumoral cell proliferation [23]. The inhibition of SAC will reduce cancer cell proliferation or cancer cell death, making 2x93 a new approach to selectively target cancer cells. Ras family small GTPases/proteins are one of the focal points in a cancer research because of their role as "on/off switch" signaling pathways. They include 3kkp and 5p21. They control cellular signaling pathways responsible for growth, migration, adhesion, cytoskeletal integrity, survival and differentiation. As a result, multiple approaches are undertaken to develop tumor therapies efficiently targeting RAS and RAS effector pathways [24].

The initial preparation of the pdb files to select the needed chains, delete multiple ligands and non-protein parts were done using Discover Studio visualize [25] version 16. 1.0. 15350. The 2D and 3D structures of the ligands were drawn using ACD/ChemSketch 2015 version [26]. OpenBabel [27] GUI version 2.3.2 and AutoDock [28] were used to convert the pdb file to pdbqt format. AutoDock Tools 1.5.6 and AutoDock Vina version 1.1.2 (downloaded from http://autodock.scripps.edu) were used for molecular docking process [29]. Discover Studio visualize [26] version 16.1.0.15350 was used for analyzing docking results [30].

2.2. Synthesis of 3-Chloro-10*h*-pyrido[3,2-b][1,4]benzothiazine 7

In a 250 ml flask containing sodium hydroxide (1.79 g, 3 mmol) in 50 ml of water was added 2-aminothiophenol (2 g, 2 mmol) and entire mixture warmed until reagents dissolved. Thereafter, freshly prepared 2,3,5-trichloropyridine (2.92 g, 1.6 mmol) in 50 ml of DMF was added in drops within 15 min and the mixture boiled for 4 h. The reaction mixture at the end was filtered and the residue was washed with cold water. The obtained solid product was dried and recrystallized from ethanol to yield a yellow colored compound. Yield 7.90 g (65 %), m.p. 375–376 K. UV-Visible λ_{max} (ethanol): 280 (4.55), 310 (4.40), 350 (3.93). FT-IR (cm^{-1}) (KBr): 3438 (N-H), 3049 (Ar-H), 1615 (C=C), 1356–1315 (C-N). δ_H (400 MHz $CDCl_3$): 7.82 (1H, s, br, N-H), 7.6–6.8 (6H, m, Ar-H). δ_c (100 MHz $CDCl_3$): 144.19, 140.39, 138.98, 120.39, 118.20, 115.57, 110.33, 106.02. (Anal. calcd. for $C_{11}H_7ClN_2S$: C, 43.34; H, 2.42. Found: C, 43.10; H, 2.60).

2.3. General Procedure for Synthesis of Benzoxazine/Benzothiazine Carboxamides

A 250 ml two-necked flask containing $NiCl_2$ (0.3 g, 2.3 mmol) and PPh_3 (0.9 g, 3.4 mmol) was fitted with a teflon septum. The vessel was evacuated and backfilled with nitrogen (three times) before degassed water (1 ml) and *tert*-butanol (2 ml) were injected into the vessel and entire mixture heated for 1 min thereafter K_2CO_3 (1.38 g, 10 mmol), 3-chloro-1-azaphenoxazine (2.18 g, 9.90 mmol), and amides (10.0 mmol) were added to the solution and entire mixture heated at 383 K for 4 h under inert atmosphere until a limiting reactant was completely consumed. The reaction was cooled to room temperature, diluted with ethyl acetate and the crude product extracted from water 3 times. The combined organic extracts were dried with $MgSO_4$, and concentrated in vacuum. The crude product was purified by a silica-gel column chromatography to afford the desired product as a light yellow solid after recrystallization from the aqueous ethyl acetate.

2.4. ***N***-(10***H***-Pyrido[3,2-b][1,4]benzothiazin-3-yl)acetamide 8

Compound **8** was obtained as a dark-grey solid after recrystallization from the aqueous ethyl acetate. Yield 43 %, m.p. 381–383 K (dec). UV-Visible λ_{max} (ethanol): 288 (4.55), 290 (4.40), 360 (3.93). FT-IR (cm^{-1}) (KBr): 3310–3250 (N-H), 3030 (Ar-H), 1708 (C=O), 1615 (C=C), 1464–1414 (C=N), 1356–1305 (C-N), 832, 754 (mono substituted benzene ring). δ_H (400 MHz $CDCl_3$): 8.78 (s, br, 1H, HNCO), 7.81 (1H, s, br, N-H), 7.6–6.8 (6H, m, Ar-H), 2.4 (3H, s, CH_3-). δ_c (100 MHz $CDCl_3$): 184.19 (C=O), 140.39, 138.98, 120.39, 118.20, 115.57, 110.33, 106.02, 32.00. (Anal. calcd. for $C_{13}H_{11}N_2OS$: C, 60.68; H, 4.31. Found: C, 60.49; H, 4.50).

2.5. ***N***-(10***H***-Pyrido[3,2-b][1,4]benzothiazin-3-yl)benzamide 9

Compound **9** was obtained as a dark ash solid after recrystallization from the aqueous ethyl acetate. Yield 32 %, m.p. 361–363 K (dec). UV-Visible λ_{max} (ethanol): 216 (4.78), 254 (4.80), 309 (4.46), 475 (4.06). FT-IR (cm^{-1}) (KBr): 3350–3307 (N-H), 3161–3070 (Ar-H), 1660 (C=O), 1615 (C=C), 1484–1425 (C=N), 1356–1225 (C-N), 893 (monosubstituted aromatic ring). δ_H (400 MHz $CDCl_3$): 8.50 (1H, s, HNCO), 7.81 (1H, s, br, N-H), 7.60–6.85 (11H, Ar-H), 4.24 (s, 1H, -NH-). δ_c (100 MHz $CDCl_3$): 177 (C=O), 154.19, 148.39, 141.98, 130.59, 128.20, 122.34, 115.57, 110.33, 106.02. (Anal. calcd. for $C_{13}H_{11}N_2OS$: C, 60.68; H, 4.31. Found: C, 60.49; H, 4.50).

2.6. 4-Nitro-***N***-(10***H***-pyrido[3,2-b][1,4]benzothiazin-3-yl)benzamide 10

Compound **10** was obtained as a light yellow solid after recrystallization from the aqueous ethyl acetate. Yield 40 %, m.p. 375–377 K (dec). UV-Visible λ_{max}(ethanol): 212 (3.40), 251 (4.93), 306 (4.40), 404 (2.88). FT-IR (cm^{-1}) (KBr): 3400–3310 (N-H), 3040 (Ar-H), 1690 (C=O), 1610 (C=C), 1405 (C=N), 1356–1305 9 (C-N). δ_H (400 MHz $CDCl_3$): 10.2 (1H, s, HNCO), 8.22 (1H, s, br, N-H), 7.53–6.61 (10H, m, Ar-H). δ_c(100 MHz $CDCl_3$): 175.20 (C=O), 149.11, 143.30, 138.18, 132.39, 128.20, 120.34, 115.57, 110.33, 106.02. (Anal. calcd. for $C_{18}H_{12}N_4O_3S$: C, 59.33; H, 3.32. Found: C, 59.49; H, 3.30)

2.7. 2-(10***H***-Pyrido[3,2-b]benzothiazin-3-yl)-2,3-dihydroisoquinoline-1,4-dione 11

Compound **11** was obtained as a light yellow solid after recrystallization from the aqueous ethyl acetate. Yield 42 %, m.p. 379–381 K (dec). UV-Visible λ_{max}(ethanol): 201 (4.55), 251 (4.03), 320 (4.40), 424 (2.98). FT-IR (cm^{-1}) (KBr): 3450–3320 (N-H), 3040 (Ar-H), 1720, 1698 (C=O), 1610 (C=C), 1405 (C=N), 1356–1335 (C-N). δ_H (400 MHz $CDCl_3$): 8.72 (1H, s, br, N-H), 8.11–7.25 (8H, m, Ar-H), 2.18–2.32 (2H, s, -CH_2-). δ_c (100 MHz $CDCl_3$): 181.23, (C=O), 147.11, 145.30, 140.28, 135.30, 130.20, 125.14, 120.52, 115.03, 106.02, 40.34. (Anal. calcd. for $C_{20}H_{13}N_3O_2S$: C, 66.84; H, 3.65. Found: C, 66.79; H, 3.50).

2.8. 1,3-di-10***H***-Pyrido[3,2-b][1,4]benzothiazin-3-ylurea 12

Compound **12** was obtained as a light yellow solid after recrystallizatiom from the aqueous ethyl acetate. Yield 40 %, m.p. 369–371 K (dec). UV-Visible λ_{max} (ethanol): 247 (2.10), 351 (2.43), 451 (3.40), 520 (3.05). FT-IR (KBr, cm^{-1}): 3411–3355 (N-H), 3051 (Ar-H), 1684 (C=O), 1613 (C=C), 1474–1405 (C=N), 1356–1305 (C-N). δ_H (400 MHz $CDCl_3$): 10.4 (2H, s, br, HNCO), 8.22 (2H, s, NH), 7.5–6.8 (12H, m, Ar-H). δ_c(100 MHz $CDCl_3$): 171.20 (C=O), 150.21, 145.30, 138.10, 135.33, 130.20, 135.30, 125.97, 120.33, 116.12. (Anal. calcd. for $C_{23}H_{16}N_6OS_2$: C, 60.51; H, 3.53. Found: C, 60.40; H, 3.62).

Table 1

Amidation of 3-chloro-10*H*-pyrido[3,2-b]benzoxazine and 3-chloro-10*H*-pyrido[3,2-b]benzothiazine

Entry	Oxazine/thiazine	Amide	Product
1	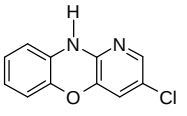 **1**	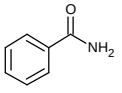	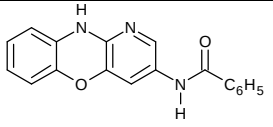 **2**
2	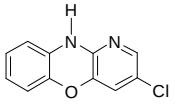	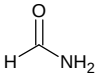	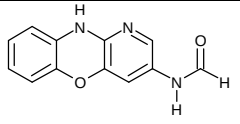 **3**
3	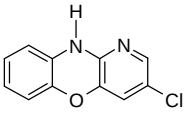	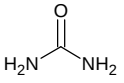	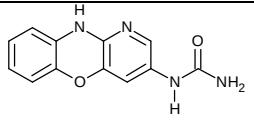 **4**
4	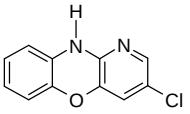	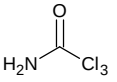	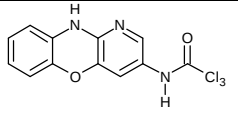 **5**
5	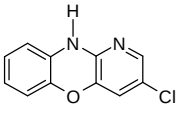	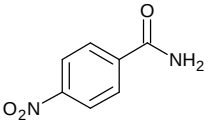	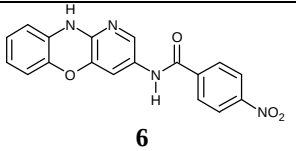 **6**
6	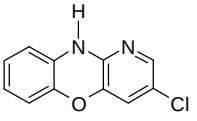		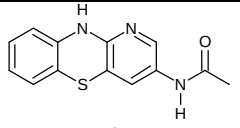 **8**
7	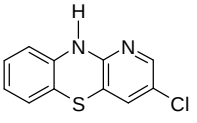 **7**	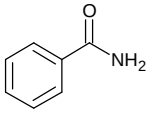	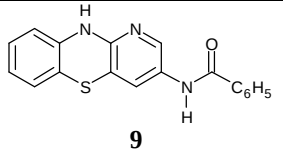 **9**
8	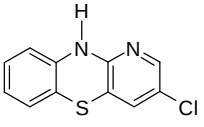	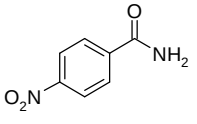	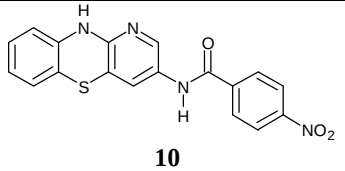 **10**
9	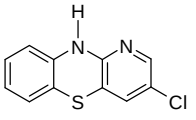	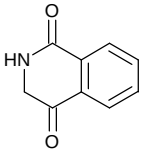	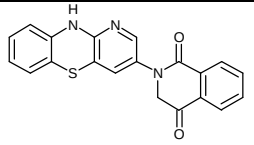 **11**
10	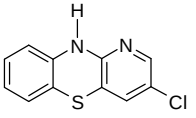	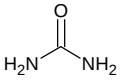	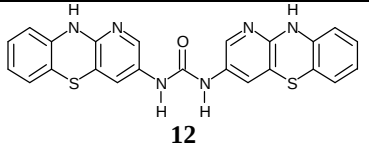 **12**

Reaction conditions: $NiCl_2$ (0.3 g, 2.3 mmol) and PPh_3 (0.9 g, 3.4 mmol), water (1 ml) and *tert*-butanol (2 ml), K_2CO_3 (1.38 g, 10 mmol), 3-chloro-1azaphenoxazine (9.90 mmol), and amides (10.0 mmol).

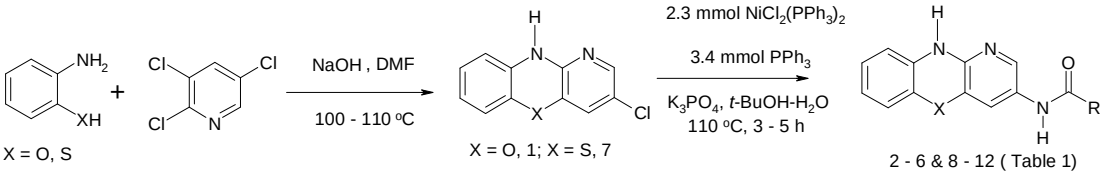

Fig. 1. Synthesis of 3-chlorophenoxazine and 3-chlorophenothiazine amido derivatives

3. Results and Discussion

3.1. Synthesis of Amido Derivatives of Phenoxazine and Phenothiazine

The intermediate compounds, 3-chloro-10*H*-pyrido[3,2-b]benzoxazine **1** and 3-chloro-10*H*-pyrido[3,2-b]benzothiazine **7** were prepared by the anhydrous base catalyzed reaction in DMF or dioxane of 2-aminophenol and 2-aminothiophenol with 2,3,5-trichloropyridine at 373 K respectively to afford yellowish powdered products in good yields after recrystallization from the aqueous ethanol (Fig. 1) [31, 32].

The cross-coupling of compounds **1** and **7** with a variety of amides *via* Ni-PPh_3 mediation afforded the 3-amido derivatives (**2-6** and **8-12)** (Fig. 1, Table 1). The synthesis and characterization of compounds **1** and **2-6** were earlier reported [17] while newly synthesized compounds **7-12** were obtained as yellowish solids in moderate isolated yields.The UV-visible data of compounds **9-12** showed bathochromic shifts as a result of extended conjugation in their molecular structures. The characteristic IR frequencies of N–H and C=O functionalities were found at 3400–3100 and 1700–1640 cm^{-1}, respectively for compounds **7-12**. The proton nuclear magnetic spectra gave broad singlet signals for N–H and HNCO protons correspondingly in such a way N–H protons were located at higher field than HNCO for all the derivatives. The assigned structures of the synthesized compounds were in agreement with other spectral and analytical data.

3.2. *In - Silico* Physicochemical Evaluation

Table 2 contains Lipinski properties such as molecular weight (MW), partition coefficient value (Log P), number of hydrogen bond donor (HBD), hydrogen bond acceptor (HBA) rotatable bonds (NoRB), total polar surface area (TPSA) and other parameters for 3-chloro-10*H*-pyrido[3,2-b]benzoxazine **1**, 3-chloro-10*H*-pyrido [3,2-b]benzothiazine **7** and their amido derivatives.

In accordance with Lipinski's rule of five, a drug must have a molecular weight value of ≤500, hydrogen bond donor ≤5, hydrogen bond acceptor ≤10 and partition coefficient (Log P) ≤5 [20]. Table 2 shows that the synthesized compounds passed the Lipinski's rule of five. The polar surface area (PSA) which is an indicator of the ligand hydrophilicity plays an important role in the protein-ligand interaction. Veber *et al.* [33] showed that 10 or fewer rotatable bonds and polar surface area, PSA ≤140 $Å^2$ would have a high probability of good oral bioavailability in rats. In addition, compounds **1, 3, 5, 7, 8, 9** and **11** were found to have PSA ≤90 $Å^2$ and so can cross the BBB and penetrate the CNS [25]. Pluta [1] noted that the biological activity of phenothiazine derivatives is a result of interaction of pharmacophoric substituents and multicyclic ring (pi-pi interaction, intercalation in DNA) as well as the penetration of biological membrane is a result of the lipophilic character of the molecule.

Table 2

***In-silico* physicochemical properties of the studied compounds**

Compound	MW	Log P	HBD	HBA	nViolation	TPSA	NoRB	Volume
1	218.64	3.29	1	3	0	41.82	0	175.38
2	303.32	3.51	2	5	0	70.92	2	264.64
3	227.22	1.86	2	5	0	70.92	1	193.23
4	242.24	1.75	4	6	0	96.94	1	204.51
5	344.58	3.64	2	5	0	70.92	2	250.34
6	348.32	3.46	2	8	0	116.75	3	287.97
7	234.71	3.94	1	2	0	28.68	0	184.52
8	257.32	2.48	2	4	0	57.78	1	218.93
9	319.39	4.15	2	4	0	57.78	2	273.78
10	364.39	4.11	2	7	0	103.61	3	297.11
11	359.41	3.73	1	5	0	66.06	1	299.10
12	456.56	5.78	4	7	1	98.49	2	373.12

Notes: MW – molecular weight; NoRB – number of rotatable bonds; P – partition coefficient; HBA – number of hydrogen bond acceptors; HBD – number of hydrogen bond donors, nViolation – number of violation; TPSA – total polar surface area.

3.3. Molecular Docking Calculations

The docking study was performed using the AutoDock Tools and AutoDock vina. 3-chloro-10*H*-pyrido [3,2-b]benzoxazine **1**, 3-chloro-10*H*-pyrido[3,2-b]benzothiazine **7** and their amido derivatives were docked into the active sites of the selected cancer target proteins.

All the compounds docked showed significant binding affinities with each of the five proteins. The interactions of compounds **11** and **12** with the receptors 3kkp, 5p21, 2x9e and 1gs4 elicited higher binding affinities than the standard drug. In addition, compounds **6** and **12** showed better interaction and higher binding affinities with the receptor 3pp1 than the standard drug (Table 3).

Compound **12,** 1,3-di-10*H*-pyrido[3,2-b][1,4]benzothiazin-3-ylurea showed the best interaction and the the highest anticancer activity with all the receptors than other derivatives. Particularly, compound **12** showed highest activity with 5p21 and 1gs4 (-11.5 and 11.2 kcal/mol, respectively). These binding energies were significantly high compared to the standard drug (methotrexate). Therefore, compound **12** with the highest binding affinity was selected to illustrate further their binding modes with 5p21 and 1gs4 (Figs. 2 and 3). A careful look at receptor-compound interaction of **12** shows the following interactions of amino acid residues of the receptors (1gs4 and 5p21**)** and the pharmacophoric atoms of the ligand **12:** hydrogen bond, aromatic pi-alkyl, aromatic pi-sulphur, Van der Waals, pi-lone pair and pi-donor hydrogen bond interactions (Figs. 4 and 5). The distances of their interactions in Å are also given.

Table 3

Binding affinity of different compounds with cancer target proteins

Compound	3kkp	Binding energy (Δ*G*), kcal/mol			
		2x9e	5p21	1gs4	3pp1
1	-6.9	-6.8	-7.3	-8.1	-7.2
2	-8.2	-7.7	-9.5	-8.5	-10.0
3	-7.1	-6.9	-8.2	-7.5	-7.6
4	-7.4	-6.9	-8.4	-8.2	-8.2
5	-7.7	-6.9	-8.5	-7.6	-8.3
6	-8.5	-8.0	-9.2	-8.5	-10.3
7	-6.5	-6.6	-6.9	-7.6	-7.1
8	-7.0	-6.7	-7.6	-7.6	-7.9
9	-7.9	-7.7	-8.3	-8.1	-8.7
10	-8.2	-8.0	-8.7	-8.0	-9.5
11	-8.8	-8.8	-9.8	-8.9	-9.7
12	-8.8	-10.0	-11.5	-11.2	-10.9
MTX	-8.2	-7.7	-9.4	-7.8	-8.7

Note: MTX – methotrexate

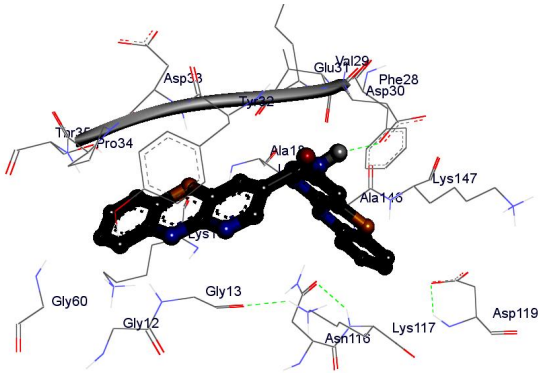

Fig. 2. Binding mode of **12** with amino acid residues of the 5p21

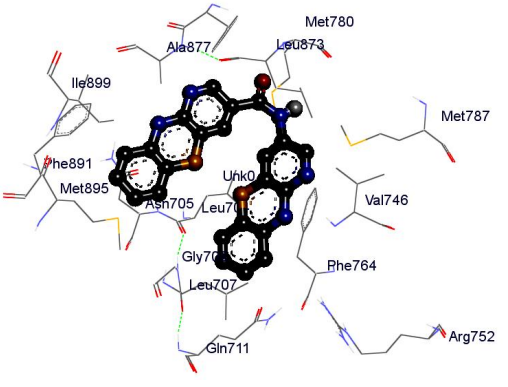

Fig. 3. Binding mode of **12** with amino acid residues of the 1gs4

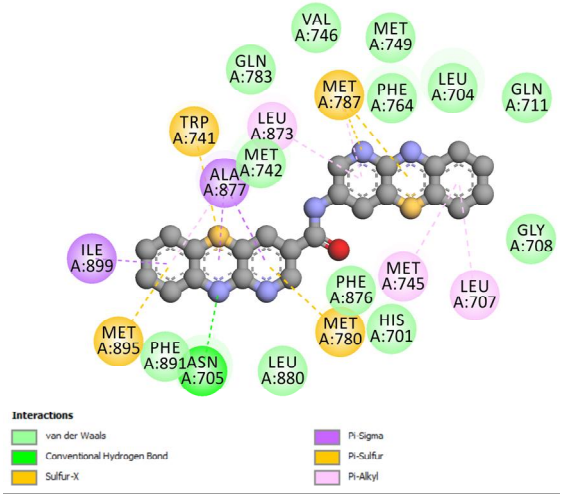

Fig. 4. Interactions of **12** with amino acid residues of the 1g4s

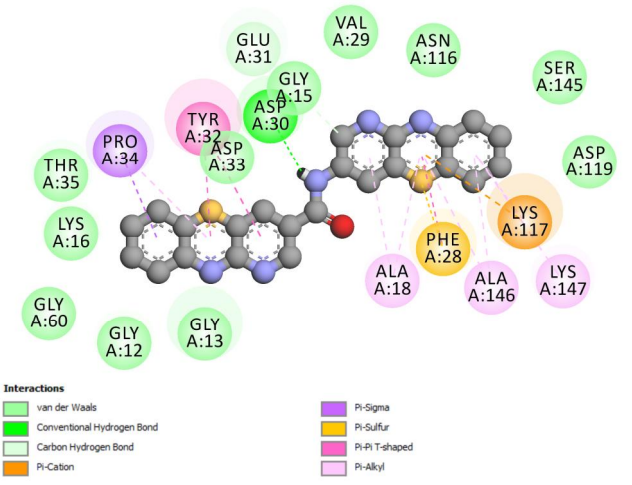

Fig. 5. Interactions of **12** with amino acid residues of the 5p21

It is worthy to note that each of the synthesized compounds was able to interact with each of the cancer target proteins, inhibiting their biochemical processes. This shows that the compounds can act as anticancer agents at different targets, interrupting essential biochemical pathways for the survival of the cancer cells, and ultimately lead to their deaths. In all the receptors used, it was observed that replacement of the chlorine atom in compound **1** and **7** with amido moieties gave rise to compounds with better binding affinities. Particularly, derivatives with benzamido group such as **2**, **6**, **9**, **10**, **11** and **12** possess higher binding affinities than other compounds without the aromatic ring in the amido group. This may be attributed to the ability of the aromatic ring to form pi interactions with sigma, alkyl and sulphur of the amino acid residues of the target proteins.

4. Conclusions

3-amido derivatives of 3-chloro-10*H*-pyrido[3,2-b][1,4]benzoxazine and 3-chloro-10*H*-pyrido[3,2-b][1,4]benzothiazine exhibited a good interaction with cancer receptors. 1,3-di-10*H*-Pyrido[3,2-b][1,4]benzo-thiazin-3-ylurea (compound **12**) possesses the highest anticancer activity, showing the significant interaction with all the receptors employed in the docking. The results from physicochemical and molecular docking studies of derivatives need to be validated by experimental data.

Acknowledgments

We thank Pharm U. S. Onoabedje for proof reading the manuscript.

References

[1] Pluta K., Morak-Mlodawska B., Jelen M.: Eur. J. Med. Chem., 2011, **46**, 3180. https://doi.org/10.1016/j.ejmech.2011.05.013
[2] Aaron J., Gaye Seye M., Trajkovska S. *et al.*: Top. Heterocycl. Chem., 2009, **16**, 202. https://doi.org/10.1007/7081_2008_125
[3] Motohashi N., Sakagami H., Kamata K., Yamamoto Y.: Anticancer Res., 1991, **11**, 1933.
[4] Pluta K., Jelen M., Morak-Mlodawska B. *et al.*: Pharmacology Rep., 2010, **62**, 319. https://doi.org/10.1016/S1734-1140(10)70272-3
[5] Miyano-Kurosaki N, Ikegami K., Kurosaki K. *et al.*: J. Pharmacol. Sci., 2009, **110**, 87. https://doi.org/10.1254/jphs.08347FP
[6] Thimmaiah K., Horton K., Seshadri R. *et al.*: J. Med. Chem., 1992, **35**, 3358. https://doi.org/10.1021/jm00096a009
[7] Shimizu S., Suzuki M., Tomoda A. *et al.*: Tohoku J. Exp. Med., 2004, **203**, 47.
[8] Kato S., Shirato K., Imaizumi K. *et al.*: Oncol. Rep., 2006, **15**, 843.
[9] Azuine M., Tokuda H., Takayasu J. *et al.*: Pharmacol. Res., 2004, **49**, 161. https://doi.org/10.1016/j.phrs.2003.07.014
[10] Onoabedje E., Ibezim A., Okafor S. *et al.*: PLoS ONE, 2016, **11**, e0163467. https://doi.org/10.1371/journal.pone.0163467
[11] Ghorab M., Alsaid M., Al-Dosary M. *et al.*: Chem. Cent. J., 2016, **10**, 1. https://doi.org/10.1186/s13065-016-0148-1
[12] Ullah M.: Asian Pacific J. Cancer Prev., 2008, **9**, 1.
[13] Fors B., Dooleweerdt K., Zeng Q. *et al.*: Tetrahedron, 2009, **65**, 6576. https://doi.org/10.1016/j.tet.2009.04.096
[14] Brett P., Philip K., Strieter F. *et al.*: Org. Lett., 2008, **10**, 3505. https://doi.org/10.1021/ol801285g
[15] Yin J., Buchwald S.: Org. Lett., 2000, **2**, 1101. https://doi.org/10.1021/ol005654r
[16] Buchwald S., Yin J.: Tetrahedron, 2009, **65**, 6576. https://doi.org/10.1016/j.tet.2009.04.096
[17] Agbo S., Anoh V., Okoro U.: J. Applicable Chem., 2014, **3**, 2526.
[18] Shima F., Ijiri Y., Muraoka S. *et al.*: J. Biol. Chem., 2010, **285**, 22696. https://doi.org/10.1074/jbc.M110.125161
[19] Colombo R., Caldarelli M., Mennecozzi M. *et al.*: J. Moll. Cancer Res., 2010, **70**, 10255. https://doi.org/10.1158/0008-5472.CAN-10-2101

[20] Pai E., Krengel U., Petsko G. *et al.*: EMBO J., 1990, **9**, 2351. https://doi.org/10.1002/j.1460-2075.1990.tb07409.x
[21] Matias P., Carrondo M., Coelho R. *et al.* J. Med. Chem., 2002, **45**, 1439. https://doi.org/10.1021/jm011072j
[22] Dong Q., Dougan D., Gong X. *et al.*: Bioorg. Med. Chem. Lett., 2011, **21**, 1315. https://doi.org/10.1016/j.bmcl.2011.01.071
[23] Colombo R., Caldarelli M., Mennecozzi M.: Cancer Res., 2010, **70**, 10255. https://doi.org/10.1158/0008-5472.CAN-10-2101
[24] Rajalingam K., Schreck R., Rapp U., Albert S.: Biochim. Biophys. Acta, 2007, **1773**, 1177. https://doi.org/10.1016/j.bbamcr.2007.01.012
[25] Dassault Systèmes BIOVIA, Discovery Studio Modeling Environment, Release 2017, San Diego: Dassault Systèmes, 2016.
[26] ACD/ChemSketch (Freeware), version 15.01, Advanced Chemistry Development, Inc., Toronto, ON, Canada, www.acdlabs.com, 2015.
[27] Boyle N., Banck M., James C. *et al.*: J. Chemoinform., 2011, **3**, 33. https://doi.org/10.1186/1758-2946-3-33
[28] Morris G., Huey R., Lindstrom W. *et al.*: J. Comput. Chem., 2009, **16**, 2785. https://doi.org/10.1002/jcc.21256
[29] Trott O., Olson A.: J. Comput. Chem., 2010, **31**, 455. https://doi.org/10.1002/jcc.21334
[30] The PyMOL Molecular Graphics System, Version 1.8 Schrödinger, LLC.
[31] Okafor C., Castle R., Wise Jr. D.: J. Heterocyclic Chem., 1983, **20**, 1047. https://doi.org/10.1002/jhet.5570200441
[32] Okafor C., Uche I., Akpanisi L.: J. Heterocyclic Chem., 1981, **18**, 1589. https://doi.org/10.1002/jhet.5570180820
[33] Veber D., Stephen R., Hung-Yuan C. *et al.*: J. Med. Chem., 2002, **45**, 2615. https://doi.org/10.1021/jm020017n

Received: February 02, 2018 / Revised: April 26, 2018 / Accepted: October 15, 2018

СИНТЕЗ І ТЕОРЕТИЧНІ ПРОТИПУХЛИННІ ДОСЛІДЖЕННЯ ДЕЯКИХ НОВИХ МОНОАЗА-10*Н*-ФЕНОТИАЗИНОВИХ ТА 10*Н*-ФЕНОКСАЗИНОВИХ ГЕТЕРОЦИКЛІВ

Анотація. *Синтезовано ряд нових 3-амінопохідних 3-хлор-10Н-піридо[3,2-b][1,4]бензоксазину та 3-хлор-10Н-піридо[3,2-b][1,4]бензотіазину та визначено їх протипухлинну активність. Синтезовані сполуки проаналізовані УФ-, 1Н ЯМР-спектроскопією, спектроскопією Фур'є та елементним аналізом. На основі фізико-хімічних властивостей за методом in silico виявлено, що проміжні продукти 3-хлор-10Н-піридо[3,2-b][1,4]бензоксазину і 3-хлор-10Н-піридо[3,2-b][1,4]бензотіазину, та їх карбоксиамідні похідні не порушують правила Ліпінського. За допомогою молекулярного докінгу показано, що синтезовані сполуки непогано взаємодіють з рецепторами раку. Визначено, що найвищу протипухлинну активність має 1,3-ді-10Н-піридо[3,2-b][1,4]бензотіазин-3-ілсечовина.*

Ключові слова: *синтез, феноксазин, фенотіазин, карбоксиамід, протипухлинні засоби, докінг.*